Electronic structure of SiC(0001) surfaces studied by two-photon photoemission

Michael Wiets, Martin Weinelt, and Thomas Fauster*
Lehrstuhl für Festkörperphysik, Universität Erlangen-Nürnberg, Staudtstr. 7, D-91058 Erlangen, Germany
(Received 26 March 2003; revised manuscript received 27 May 2003; published 24 September 2003)

Two-photon photoemission has been used to study the electronic structure of the valence and conduction bands at SiC(0001) surfaces. The various surface reconstructions show distinctly different spectra and work functions. The ionization energy is found independent of polytype and surface reconstruction to be 6.9 ± 0.2 eV. For the $(\sqrt{3}\times\sqrt{3})R30°$ surface the occupied and unoccupied Mott-Hubbard bands are found with a splitting $U=2.4\pm0.1$ eV. A long-lived exciton between the Mott-Hubbard bands is identified with a binding energy of ~0.7 eV.

DOI: 10.1103/PhysRevB.68.125321 PACS number(s): 73.20.At, 79.60.Bm, 71.20.Nr

I. INTRODUCTION

Silicon carbide is a wide-band-gap semiconductor with interesting possibilities for demanding applications, e.g., at high temperatures. An intriguing property of the material is the polytypism, which leads to different band gaps depending on the stacking sequence of the SiC bilayers.[1] The difficulties in growing a particular polytype or heterojunctions from different polytypes spurred considerable efforts in basic research on the surface properties. The hexagonal surfaces of SiC show reconstructions that reduce the number of dangling bonds compared to a truncated bulk surface.[2] For the Si-terminated SiC(0001) surfaces the reconstruction changes from (3×3) via $(\sqrt{3}\times\sqrt{3})R30°$ to $(6\sqrt{3}\times6\sqrt{3})R30°$ with decreasing Si content at the surface. All of the corresponding unit cells contain an odd number of electrons. One would expect therefore a metallic surface, which is found only for the case of the $(6\sqrt{3}\times6\sqrt{3})R30°$ reconstruction. The (3×3) and $(\sqrt{3}\times\sqrt{3})R30°$ surfaces show a band gap that is due to the splitting of the half-filled surface band into one occupied and one unoccupied Mott-Hubbard band.[3,4] The separation of these bands is given by the on-site Coulomb repulsion U, which should be large compared to the bandwidth for the splitting to occur.[5,6]

The Mott-Hubbard bands have been studied in particular on the SiC(0001)$(\sqrt{3}\times\sqrt{3})R30°$ surface with a wide variety of experimental[3,7–9] and theoretical[4–6,10] techniques. A consistent picture of the energies and dispersion of the Mott-Hubbard bands has evolved. The aim of our work was to employ two-photon photoemission (2PPE) to characterize this system. The advantage of this method is the possibility for studying both occupied and unoccupied states with one spectroscopy. The relevant processes are sketched at the right-hand side of Fig. 1. Electrons from the occupied Mott-Hubbard band at energy E_o are emitted after the absorption of two photons. The unoccupied Mott-Hubbard band at E_u is populated after absorption of one photon by an electron from the valence band. The second photon lifts the electron above the vacuum energy E_{vac}. The emitted electrons can be analyzed according to their kinetic energy E_{kin} and direction with high resolution. The unique advantage of 2PPE is the possibility for studying dynamic processes by introducing a suitable delay between the pump and probe laser pulses with femtosecond resolution.[11] The first step in 2PPE makes a neutral excitation of an electron from an occupied to an unoccupied state. This offers the chance to observe the interaction between the electron and the hole, which includes excitonic and spin-correlation phenomena. Most other experimental techniques extract or add electrons and measure therefore the bare Mott-Hubbard bands. Two-photon photoemission is particularly sensitive to surface states[11,12] and the application to the study of the Mott-Hubbard states seems worthwhile.

In this presentation of the two-photon photoemission study of SiC surfaces, we present and discuss the data in considerable detail after a short description of the experimental setup. A complete characterization of the various peaks requires measurements as a function of energy, intensity, and polarization of the photons as well as of polytype, reconstruction, and temperature of the samples. Vacuum ultraviolet photoelectron spectroscopy (UPS) complements the results with regard to the work function and the dispersion of the occupied Mott-Hubbard band. Because our experimental setup is optimized for low kinetic energies, we provide accurate results for the work function Φ, the ionization energy ξ, and the electron affinity χ (see Fig. 1) as a function of polytype and surface reconstruction. These data are of importance for the evaluation of Schottky barrier heights in technological applications.[13] The final section of the results discusses the exciton between the Mott-Hubbard bands.

II. EXPERIMENT

The experimental requirements for two-photon photoemission are a laser system as the excitation source and an electron energy analyzer. The latter is housed in an ultrahigh vacuum system that is also used for the *in situ* sample preparation. Electrons were detected by an electrostatic hemispherical analyzer (Omicron EA 125 HR) with an acceptance cone of $\pm1.5°$. The energy resolution was tuned to 35 meV and a small bias of 1 eV (3 eV for normal emission $\vartheta=0°$) was applied between sample and analyzer. In order to achieve high sensitivity at low kinetic energies a custom-made lens supply was used. In addition to the screening by the mu-metal chamber the magnetic fields were compensated by a set of Helmholtz coils. The spectra are displayed as a function of the kinetic energy with respect to the analyzer.

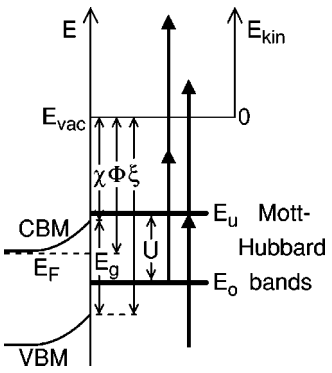

FIG. 1. Energy diagram of the SiC(0001)$(\sqrt{3}\times\sqrt{3})R30°$ surface illustrating two-photon photoemission processes involving the Mott-Hubbard states.

Reference to the Fermi energy E_F common to sample and analyzer is made by adding the analyzer work function of 4.32 eV. The latter was measured with an accuracy of 0.02 eV from the high-energy cutoff of UPS spectra (see curve for the Pt sample holder in Fig. 2) using the known photon energy of 21.22 eV of the He I radiation.

The laser setup[14] consists of a home-built Ti:sapphire laser pumped by a 5 W diode-pumped solid-state laser (Spectra Physics, Millennia). The infrared (ir) pulse length at 790 nm is 12 fs at a repetition rate of 87 MHz. Introducing a slit in the cavity increases the pulse length to 23 fs, but allows wavelength tuning between 750 and 820 nm (850 nm with a different set of mirrors). 10% of the output power of 560 mW was sent after pulse compression directly to the sample. The major part was used to generate the third harmonic of the ir radiation. The power of the frequency-tripled beam in the ultraviolet (uv) at 263 nm (253 nm) was 10 mW (2.5 mW). After pulse compression the cross-correlation between the uv and ir beam was measured to 46 fs by monitoring the 2PPE signal from the occupied surface state at a Cu(111) sample.[15] Using the longer ir pulses increased the conversion efficiency of the frequency tripler without any significant increase of the cross-correlation width compared to shorter ir pulses. For time-resolved measurements involving two uv pulses, the uv beam was split and recombined in a Mach-Zehnder type interferometer. Note that only half of the uv intensity is available at the sample in this configuration. The cross-correlation is dominated by interference effects, which are difficult to resolve with a mechanical delay stage at the wavelength of 263 nm. The angle between the incident beams and the electron detection was 45°. The polarization of uv and ir light could be changed independently by quarter-wave plates. Data were collected with *p* polarization for both beams unless stated otherwise.

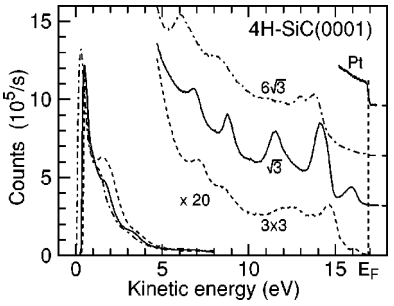

FIG. 2. Photoemission spectra for different reconstructions of a 4*H*-SiC(0001) surface.

The sample preparation followed the widely accepted standard procedure[2] of Si evaporation at 800 °C for 30 min to produce the (3×3) reconstructed surface. Heating to 1000 °C for 30 to 120 min leads to the $(\sqrt{3}\times\sqrt{3})R30°$ reconstruction and after annealing at 1100 °C for 10 min the $(6\sqrt{3}\times6\sqrt{3})R30°$ surface is obtained. With fresh Si evaporation a new preparation cycle can be started. The type and quality of the reconstructions were checked by low-energy electron diffraction (LEED), x-ray photoelectron spectroscopy (XPS) of the Si $2p$ and C $1s$ core levels, UPS using the He I resonance line, and the 2PPE spectra. For reproducible results the samples were flashed to 800 °C for 1 min to desorb contaminations from the residual gas (base pressure 3×10^{-11} mbar), which consisted mainly of hydrogen. Due to the large copper mass of the manipulator, the sample reached the measuring temperature within a few minutes, in particular when the manipulator was cooled with liquid nitrogen.

III. RESULTS

A. Vacuum ultraviolet photoemission

1. Spectra for different reconstructions

Photoemission using the He I line of a discharge lamp was used to characterize the sample preparation. Spectra for the (3×3), $(\sqrt{3}\times\sqrt{3})R30°$, and $(6\sqrt{3}\times6\sqrt{3})R30°$ reconstructed surfaces are shown in Fig. 2. Pronounced differences are observed in the surface states ($E_{kin}>15$ eV), the valence-band features ($5<E_{kin}<15$ eV), and the position of the low-energy cutoff. The peaks are best developed for the $(\sqrt{3}\times\sqrt{3})R30°$ reconstruction. The lower intensity of the valence-band peaks for the two other reconstructions may be attributed to the additional Si and C atoms at the surface for the (3×3) and $(6\sqrt{3}\times6\sqrt{3})R30°$ reconstruction, respectively. For the $(\sqrt{3}\times\sqrt{3})R30°$ surface we obtain the top of the valence band at an energy of 2.3 ± 0.2 eV below E_F. The accuracy is limited by the extrapolation procedure to determine the emission from the valence-band maximum (VBM). This becomes even more cumbersome for the other reconstructions, but values similar to those for the $(\sqrt{3}\times\sqrt{3})R30°$ surface are found. Photoemission spectra show a considerable variation with photon energy near the VBM.[7] In view of the small variations of the work function upon reconstruction (see Sec. III A 2), it seems plausible to attribute the energy differences of the valence-band peaks to surface-umklapp processes of bulk bands or surface states. This is also supported by the fact that the valence-band features for different reconstructions cannot be matched by a rigid shift of the spectra. The present results are in good agreement with previous photoemission studies.[7,16–18]

2. Low-energy cutoff and work function

Our experimental setup is optimized for electron spectroscopy at low kinetic energies, which permits an accurate de-

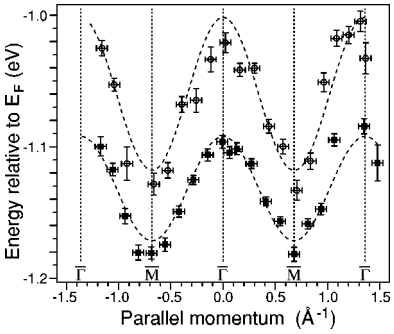

FIG. 3. Dispersion of the occupied Mott-Hubbard state on the SiC(0001)($\sqrt{3}\times\sqrt{3}$)$R30°$ surface for two different sample preparations. Dashed lines are fits to a cosine dispersion.

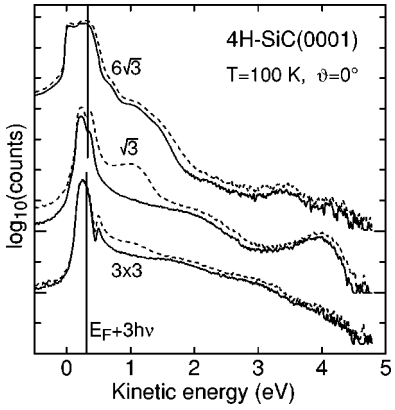

FIG. 4. Two-photon photoemission spectra of 4H-SiC(0001) for the (3×3), ($\sqrt{3}\times\sqrt{3}$)$R30°$, and $(6\sqrt{3}\times6\sqrt{3})R30°$ surface reconstructions taken with a fundamental photon energy $h\nu=1.55$ eV [1.54 eV for (3×3)]. For clarity, spectra (Ref. 20) are offset by two orders of magnitude indicated by tics on the ordinate axis. The broken line indicates the Fermi edge after $3h\nu$ excitation.

termination of the work function from the low-energy cutoff of photoemission spectra (see Fig. 2). The work functions obtained for the (3×3) and ($\sqrt{3}\times\sqrt{3}$)$R30°$ reconstructions of 4.70 ± 0.08 eV and 4.74 ± 0.06 eV are almost identical, whereas for the $(6\sqrt{3}\times6\sqrt{3})R30°$ surface a significantly smaller value of 4.49 ± 0.08 eV is found. The error of these values is mainly due to the scatter of different sample preparations. The experimental uncertainty for a single measurement is ±0.01 eV.

3. Dispersion of the occupied Mott-Hubbard state

For the ($\sqrt{3}\times\sqrt{3}$)$R30°$ reconstruction the dispersion of the occupied surface state shown in Fig. 2 was measured. The results for two different sample preparations of the ($\sqrt{3}\times\sqrt{3}$)$R30°$ 4H-SiC surface are shown in Fig. 3. The dispersion shows the expected behavior and periodicity along the $\bar{\Gamma}\,\bar{M}$ direction of the surface Brillouin zone. The bandwidth is ~0.1 eV and the mean energy varies by ±50 meV for different sample preparations. This is most likely attributed to different concentrations of Si adatoms, which depend on the evaporated amount of Si and the annealing temperature. The ($\sqrt{3}\times\sqrt{3}$)$R30°$ SiC surfaces are very sensitive to contamination from residual gas; therefore the sample was flashed to 800 °C for 1 min. Data were taken after cooling down of the sample to 100 K. Without repeated heating the periodicity of the dispersion was not clearly observed and larger values for the bandwidth would be obtained. We attribute contamination as the most likely cause for the absence of a periodic dispersion[19] and the larger bandwidths observed in previous photoemission studies (see Table II).

B. Two-photon photoemission

1. Spectra for different reconstructions

Figure 4 presents spectra for (3×3), ($\sqrt{3}\times\sqrt{3}$)$R30°$, and $(6\sqrt{3}\times6\sqrt{3})R30°$ surface reconstructions of the SiC(0001) surface in semilogarithmic plots to account for the high dynamic range of the data. The filled lines correspond to spectra, that are excited by uv light only, while the dashed curves were recorded with ir light in addition. Differences are clearly recognizable in the spectra, which are due to variations of the work function (see Table I) and the electronic surface states. Two-photon photoemission spectra show characteristic features depending on the surface reconstruction in a similar fashion as UPS data (see Fig. 2). For the $(6\sqrt{3}\times6\sqrt{3})R30°$ surface no additional peaks are found as a result of the ir light. For the other reconstructions a significant increase of the count rate around $E_{kin}=1$ eV is observed. In the following we focus on the properties of the various features for the best-ordered ($\sqrt{3}\times\sqrt{3}$)$R30°$ reconstruction.

TABLE I. Experimental values for the work function Φ and electron affinity χ for SiC(0001). All energies are in eV.

Φ	χ	Type	Doping	Method	Reference
4.40–4.62			n,p	Kelvin	28
4.62 ± 0.1		3C			29
4.75–4.85	3.7[a]	6H	n,p	Ret. field	31
	3.7–3.8	6H	n	IV/CV	32
	3.3[b]	6H	n,p		33,13
	4.7	6H			34,35
4.5		6H	n,p	Kelvin	36
	3.08 ± 0.05	4H		Ret. field	37
	3.34 ± 0.05	6H		Ret. field	37
	3.83 ± 0.02	3C		Ret. field	37
4.5 ± 0.1		6H	n	Kelvin	38,39
~4.3		6H, $\sqrt{3}$	n	UPS	40
4.8 ± 0.2		6H	p	Ret. field	41
4.70 ± 0.08	3.4 ± 0.2	4H,3×3	n	UPS,2PPE	This work
4.74 ± 0.06	3.6 ± 0.2	4H, $\sqrt{3}$	n	UPS,2PPE	This work
4.89 ± 0.05	4.0 ± 0.2	6H, $\sqrt{3}$	n	UPS	This work
4.49 ± 0.08		4H, $6\sqrt{3}$	n	UPS	This work

[a]Calculated following Ref. 30.

[b]Calculated using Φ from Ref. 31 following Ref. 30.

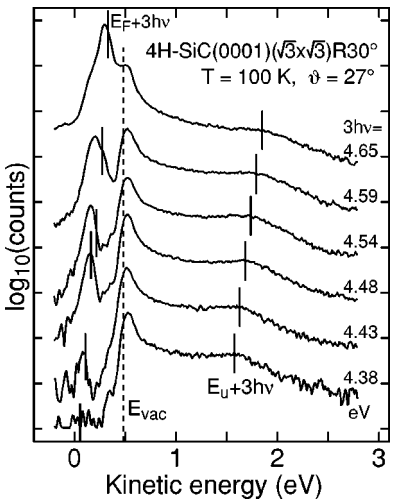

FIG. 5. Two-photon photoemission spectra of 4*H*-SiC(0001)-$(\sqrt{3}\times\sqrt{3})R30°$ with uv excitation at the indicated photon energies $3h\nu$ for an emission angle $\vartheta=27°$. For clarity, spectra (Ref. 20) are offset by one order of magnitude indicated by tics on the ordinate axis.

2. Low-energy cutoff

All spectra measured with $3h\nu=4.65$ eV are dominated by strong emission at low kinetic energies (see Fig. 4). The emission shows only a weak variation of energy position or intensity when increasing the temperature from 100 to 300 K (compare Figs. 8 and 9). Additional ir light does not increase the signal in the low-energy range. Figure 5 presents data for the $(\sqrt{3}\times\sqrt{3})R30°$ reconstruction at lower excitation energies and an emission angle $\vartheta=27°$. The onset of the spectra is below E_{vac} as determined by the threshold of the corresponding UPS measurements (see Fig. 2). The tic marks at low kinetic energies in Fig. 5 indicate the kinetic energy of electrons excited with $3h\nu$ from the Fermi energy. The low-energy emission disappears for lower photon energies and is due to one-photon photoemission from local areas of lower work function. It is not possible to quantify the size and number of these patches, but one has to keep in mind that one-photon photoemission signals are 4 to 5 orders higher than two-photon photoemission signals.[21] From this an upper limit of a few percent for these defect areas is estimated. Scanning tunneling microscope images show defects of a comparable concentration.[22] The extremely high count rates from the $(6\sqrt{3}\times6\sqrt{3})R30°$ surface (see Fig. 4) can be explained by the low work function (see Table I) and the metallic character compared to the more silicon-rich surfaces that have band gaps around E_F.

On the $(\sqrt{3}\times\sqrt{3})R30°$ surface two structures are observed in the low-energy range. The structure at ≈0.1 eV kinetic energy registers at the photon energy $3h\nu=4.65$ eV of Fig. 4 only as a shoulder; it is, however, detected at lower photon energies clearly (see Fig. 5). Since the structure does not show dispersion as function of the emission angle, it is attributed to emission out of disordered areas. A further emission peak is observed at 0.24 eV kinetic energy with onset at 0.15 eV, which behaves similarly and is also interpreted as one-photon photoemission from areas with a reduced work function (4.47 eV). At the low photon energies and sample temperatures of 100 K the intensity is increased by additional ir light. This peak disperses with increasing emission angle to higher energies (comparable to the vacuum edge discussed later). It is attributed to emission from ordered areas of the surface. It could be due to larger areas with missing adatoms, which develop in the transition to the $(6\sqrt{3}\times6\sqrt{3})R30°$ reconstruction. This interpretation is supported by the good agreement of the work function. The extent of these areas is probably so small that it cannot be recognized with LEED. However, due to the large count rates from the $(6\sqrt{3}\times6\sqrt{3})R30°$ surface (see Fig. 4) they appear as the dominant feature in the spectra of the $(\sqrt{3}\times\sqrt{3})R30°$ surface for higher photon energies.

The vacuum edge of the $(\sqrt{3}\times\sqrt{3})R30°$ reconstruction is at 0.48 eV kinetic energy. The work function of 4.8 eV, determined from this energy, corresponds to the value from the UPS spectra. The classification of this structure as vacuum edge of the ordered areas of the surface is supported by the observation of a dispersion of this feature corresponding to free electrons. In the UPS spectra no indications for areas of lower work function are found. This supports the statement that the emission with lower energies described before arises only from small areas of the surface. The used photon energies were usually smaller than the work function, so that the emission at the vacuum edge of the $(\sqrt{3}\times\sqrt{3})R30°$ reconstruction comes from unoccupied states. At 300 K sample temperature or additional ir light the signal is strongly increased (compare Figs. 5 and 8 for similar photon energies), which is due to a thermal or an electronic occupation of the states.

The energy of the vacuum edge changes little with temperature or with uv and ir light intensity. Even at high intensities of the laser sources for 2PPE no surface photovoltage develops, because due to the high doping and the small absorption by SiC (Ref. 23) only few charge carriers are generated in the space-charge layer. Note that the energetic position of the surface Fermi level seems to be very well defined independent of the preparation. This is proven also by the good agreement of the results for the surface states with other work. About the type and number of defects, which determine the Fermi level at the surface, no reliable information exists. In scanning tunneling microscopy images there are, however, characteristic defects such as missing adatoms, which occur reproducibly and in a concentration of approximately 4%.[22]

3. uv-power dependence

For the identification of the various peaks in the two-photon photoemission spectra it is important to know the number of absorbed photons. This is achieved by registering the count rate as a function of the intensity of the incident light. One-photon photoemission should show a linear dependence, whereas a quadratic behavior is characteristic for 2PPE. Spectra were taken for uv power ranging from 1 to 8 mW and the count rate was fitted to a power law[24] for each kinetic energy. The resulting exponents are shown in Fig. 6 together with the spectra taken for 8 mW. The transition from

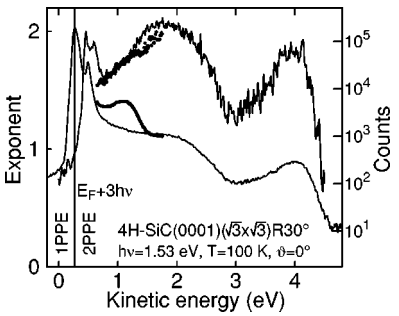

FIG. 6. Exponent of the uv power dependence of 2PPE from $4H$-SiC(0001)$(\sqrt{3}\times\sqrt{3})R30°$ (upper curve, left scale). For comparison, spectra for the highest uv power at $h\nu=1.53$ eV are shown (lower curve, right scale). In the energy range from 0.7 to 1.7 eV data with additional ir light are plotted as circles.

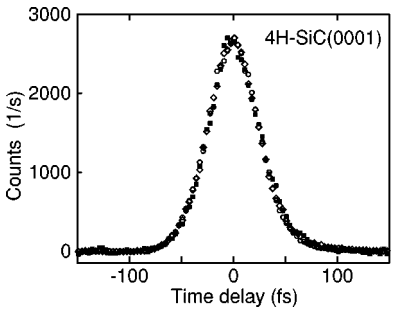

FIG. 7. Cross-correlation between the $3h\nu$ and $h\nu=1.56$ eV laser pulses. Filled and open symbols are for the peak around 1 eV kinetic energy on $4H$-SiC(0001)$(\sqrt{3}\times\sqrt{3})R30°$ and the occupied surface state on Cu(111), respectively.

one- to two-photon emission is clearly seen at a kinetic energy of 0.27 eV corresponding to $3h\nu=4.59$ eV minus the work function of the analyzer of 4.32 eV. This proves the one-photon photoemission character of the low-energy features, which must therefore arise from areas with a correspondingly low work function. For all the other peaks at higher kinetic energies the second-order process is confirmed. The dip of the exponent around 3 eV kinetic energy in Fig. 6 is probably an artifact. In this energy range no peaks are found and the emission has a considerable amount of background signal. By a suitable background subtraction the exponent can be brought close to 2 without affecting the exponent in the other energy regions significantly.

More remarkable is the dependence on uv power with additional ir light on the sample. The results for kinetic energies around 1 eV are shown by circles in Fig. 6. A value for the exponent around 1.7 is found, practically identical to the experiment without ir light. This cannot be explained by 2PPE due to uv light only, because the count rate with additional ir light is about a factor of 10 higher. The obvious and somewhat puzzling conclusion is that the peak at 1 eV kinetic energy arises predominantly after absorption of two uv photons plus one ir photon.[25] It is stunning that this three-photon photoemission process leads to a feature with such high intensity in the spectra.

4. Time-resolved measurements

The high intensity combined with the contributions from both laser pulses makes the peak at 1 eV kinetic energy an ideal candidate for time-resolved measurements. Here a time delay between ir and uv laser pulses is introduced and the intensity of the peak is recorded. For a finite lifetime of an intermediate state the sequence of the excitation steps can be identified.[11,14] Figure 7 shows the results of a time-resolved measurement on $4H$-SiC(0001)$(\sqrt{3}\times\sqrt{3})R30°$. For a precise determination of zero time delay the cross-correlation between uv and ir pulses was measured for the occupied surface state on Cu(111), which is known to have a negligible lifetime.[15] Such reference data were taken before and after the measurement on the SiC surface and show no detectable drift of the cross-correlation. Within experimental uncertainty the cross-correlation for SiC is identical to that for Cu(111). This would imply that the lifetime of a possible intermediate state is below 5 fs and no statement can be made on the excitation sequence. In the previous section (Sec. III B 3) we concluded that this transition involves a three-photon excitation process. The measurement of a negligible lifetime is only compatible with a two-step process involving the two-photon absorption of one uv and one ir photon followed (or preceded) by the absorption of another uv photon. In this case ir and uv photons have to be available at the same time to perform the first (or second) excitation step. No lifetime could be measured since no intermediate state is involved in the two-photon absorption process. An alternative possibility would be simultaneous absorption of the three photons, which seems unlikely to lead to a peak with such high intensity. Excitation into a long-lived intermediate state could lead to a high intensity in the two-step absorption process. For a final clarification of the involved processes a time delay would have to be introduced between the two uv photons, while keeping the ir pulse synchronized with one of the uv pulses, which was not possible with our experimental setup.

5. Photon-energy dependence

The power dependence identifies the number of photons absorbed. However, from energy considerations alone one- and two-photon photoemission can be separated. Additional information about the spectral features could be obtained from time-resolved measurements,[14] which was, however, inconclusive for the 1 eV peak on the SiC(0001)$(\sqrt{3}\times\sqrt{3})R30°$ surface. For a proper identification of the various 2PPE peaks, we need to know whether they arise from an occupied initial state or an unoccupied intermediate state. For two different photon energies there exist in addition several possibilities for the sequence in which the photons are absorbed.[11] A variation of the photon energy by $\Delta h\nu$ leads to a change in the kinetic energy ΔE_{kin} of the observed peaks. A slope $\Delta E_{kin}/\Delta h\nu$ of n implies that the electron was ejected after absorption of a photon with energy $nh\nu$. This applies only to surface states, for transitions between bulk bands different slopes may be observed.[11]

The photon-energy dependence of the various features observed on $4H$-SiC(0001)$(\sqrt{3}\times\sqrt{3})R30°$ is presented in Figs. 5 and 8. The two sets of data cover different photon

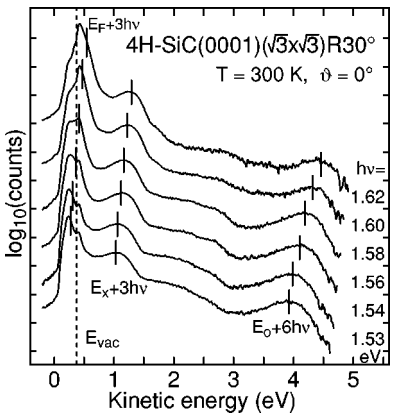

FIG. 8. Two-photon photoemission spectra of $4H$-SiC(0001)-$(\sqrt{3}\times\sqrt{3})R30°$ with uv and ir excitation at the indicated photon energies $h\nu$. For clarity, spectra (Ref. 20) are offset by one order of magnitude indicated by tics on the ordinate axis.

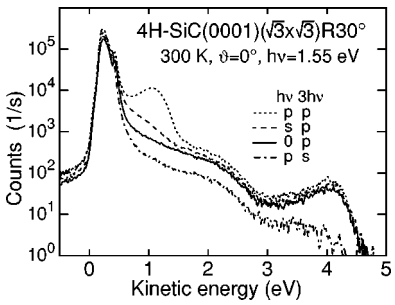

FIG. 9. Two-photon photoemission spectra of $4H$-SiC(0001) for the $(\sqrt{3}\times\sqrt{3})R30°$ reconstruction with various combinations of the polarization of the uv and ir light.

energies, but the main difference is the additional ir excitation in Fig. 8. The low-energy features do not change in position with photon energy as expected for the vacuum level of the surface (indicated by the dashed line labeled E_{vac}) or patches of different work function. The intensity variations have been discussed before in Sec. III B 2. The feature around 4 eV kinetic energy in Fig. 8 corresponds to a state around $E_F-0.95$ eV, which is excited by two uv photons of energy $3h\nu$ in agreement with the power dependence (see Sec. III B 3). This peak fits the occupied Mott-Hubbard state found in UPS (see Sec. III A) and has in both spectroscopies a peak width around 0.6 eV. The feature around 1.8 eV kinetic energy is seen more clearly as a peak for off-normal emission in Fig. 5. It correponds to an unoccupied state around $E_F+1.5$ eV, which is emitted after absorption of one uv photon. The last and most prominent feature—aside from the low-energy cutoff—is the peak around 1 eV kinetic energy, which is only seen with uv and ir light. The tic marks in Fig. 8 are plotted for an intermediate state at $E_F+0.75$ eV excited by one uv photon. This assignment is in agreement with the conclusions of Secs. III B 3 and III B 4 when the first excitation step involves the simultaneous absorption of one uv and one ir photon.

6. Polarization dependence

The polarization dependence of the spectral features yields information on the symmetry of the involved states. Spectra for various combinations of the polarization of the uv and ir light are shown in Fig. 9. For *s*-polarized uv light and *p*-polarized ir light the emission at higher kinetic energies is suppressed and no significant changes are observed with *s*-polarized or no ir light. In particular, the occupied Mott-Hubbard state around 4 eV kinetic energy cannot be observed with *s*-polarized uv light. This is in agreement with the $3p_z$ orbital character of this band.[26,27] For *p*-polarized uv light the spectra are independent of the ir light in the kinetic energy range above ~ 2 eV where only photoemission involving two uv photons is possible. The peak around 1 eV kinetic energy is present only for additional *p*-polarized ir light, which is the polarization used to obtain the spectra shown in all the other figures of this work. For *s*-polarized ir light there is additional intensity around 0.8 eV kinetic energy compared to the situation with only *p*-polarized uv light. An inspection of the data on a linear scale reveals no peak in this region. The monotonically decreasing background with increasing energy is probably due to hot electrons excited by the ir light. The features around 1 and 4 eV kinetic energy show identical behavior characteristic for totally symmetric states with respect to the surface normal, e.g., *s* or p_z orbitals. The broad structure around 2 eV is seen with both polarizations although with lower intensity for *s*-polarized uv light.

IV. DISCUSSION

A. Work function and electron affinity

1. Work function

From our photoelectron spectra we obtain the work function from the low-energy cutoff using the work function of the analyzer. There is excellent agreement between UPS and 2PPE, provided the emission from defects is identified properly in 2PPE (see Sec. III A 2). There is no significant dependence on temperature of the measured values. Our results show clearly that the work function depends on the reconstruction. The work function is ~ 0.25 eV lower for the $(6\sqrt{3}\times 6\sqrt{3})R30°$ surfaces compared to the more Si-rich (3×3) and $(\sqrt{3}\times\sqrt{3})R30°$ reconstructions, which have almost identical work functions.

Table I list measured values for the work function Φ and electron affinity χ for SiC surfaces. The large scatter of the reported values for the work function between 4.3 and 4.85 eV could be attributed to different surface preparations, which are not specified in most cases. Only the most recent studies report $(\sqrt{3}\times\sqrt{3})R30°$ reconstructions,[36,40,41] but these results also cover the range from 4.3 to 4.8 eV. A systematic study of the work function with respect to polytype under well-defined conditions has not been done so far. The work function seems to be largely independent of doping[31,36] indicating a well-defined Fermi level pinning at the surface. This is supported by the measurements of electronic states at the surfaces discussed in Sec. IV B.

In photoemission experiments the binding energies of core levels are also measured relative to E_F. The core levels

TABLE II. Experimental and calculated results for the electronic structure of the SiC(0001)$(\sqrt{3}\times\sqrt{3})R30°$ surface at $k_{\parallel}=0$.

VBM$-E_F$	E_o-E_F	U	E_u-E_F	Bandwidth	Polytype	Doping	T (K)	Method	Reference
		2.3[a]	1.10±0.05	0.34±0.05	6H	n		IPE[b]	3,53
		2.05[c]	1.0±0.1	0.1	6H	p		IPE	41
	−1.1	2.0	0.9		6H	n,p		STS	8
	−1.3				4H	n	100	UPS	44
−2.3±0.3	−1.3				6H	n	100	UPS	16
−2.3±0.2	−1.2±0.1			0.2	6H,4H	n	RT	UPS	7
∼−2.5	∼−1				6H	n		UPS	40
−2.15[d]	−1.05			0.2–0.25	3C			UPS	4
−2.0±0.2	−1.05	2.0	0.95	0.2	6H	n		UPS+IPE	6,54
	VBM+(1.05±0.1)			0.35	6H	n	100	UPS	19
−2.3±0.2	−1.10±0.03			0.1	3C	n	100	UPS	43
		2.3			6H	n	300	EELS	9
−2.3±0.2	−1.05±0.05			0.1	4H	n	100	UPS	This work
	−0.94±0.05	2.4	1.45±0.1		4H	n	100	2PPE	This work
		1.6		0.18	3C			Calc.	5
		2.1		0.2	3C			Calc.	4
		1.95		0.25, 0.30	6H			Calc.	6
		1.5			Slab			Calc.	10

[a]Using E_o from Ref. 7.
[b]IPE denotes inverse photoemission.
[c]Using E_o from Ref. 4.
[d]Using χ from Ref. 32.

should have a fixed binding energy relative to the VBM, so any change of the work function should be reflected in an opposite change of the binding energy. The binding energies of bulklike core levels are 0.3–0.4 eV larger for the $(6\sqrt{3}\times 6\sqrt{3})R30°$ reconstruction compared to the $(\sqrt{3}\times\sqrt{3})R30°$ surface on 6H- and 3C-SiC.[42,43] An earlier study reported a slightly larger difference of 0.5–0.6 eV for a 4H sample.[44] For the (3×3) surface a decrease of the binding energy by 0.1 eV compared to $(\sqrt{3}\times\sqrt{3})R30°$ has been found for 4H-SiC.[45] These changes are in good agreement with our work function data. However, the absolute energies for the bulklike Si 2p (C 1s) level on $(\sqrt{3}\times\sqrt{3})R30°$ surfaces vary between 100.4 and 101.3 eV (282.6 and 283.7 eV) in different studies.[42–46] The C 1s level is always at 182.3 ±0.1 eV higher binding energy than the Si 2p level independent of reconstruction and polytype. Therefore, we conclude that the energy calibration is accurate and the large scatter of the binding energies by ∼1 eV has to be attributed to surface preparation or contamination leading to different Fermi level pinnings.

2. Electron affinity and ionization energy

For metal contacts on *n*-doped SiC surfaces the electron affinity is the relevant quantity that determines the Schottky barrier height $\Phi_B=\Phi_M-\chi$, where Φ_M is the work function of the metal. Opposite to this Schottky limit stands the Bardeen case with $\Phi_B=E_g-\Phi_0$, where Φ_0 is the energy of the surface states pinning the Fermi level. In general, a mixture between these two extremes is found:[13]

$$\Phi_B=\gamma(\Phi_M-\chi)+(1-\gamma)(E_g-\Phi_0). \quad (1)$$

The different polytypes of SiC permit a study of the dependence of the barrier height as function of band gap and electron affinity. The ionization energy $\xi=E_g+\chi$ measures the energy needed to remove an electron from the VBM. It should depend only on the surface termination and reconstruction, because these properties are largely independent of polytype.[2,47] The electron affinity includes the reaction of the many-electron system to an added electron and depends on the band gap. Under the assumption of a constant ξ it follows from Eq. (1) that Φ_B grows with E_g and decreases with $-\chi$ as found for the limiting cases of Bardeen and Schottky. The same conclusion for the dependence of Schottky barrier height on the band gap of SiC polytypes was found in the metal-induced-gap-state model.[48] Data for Schottky barrier heights for the same metal on different SiC polytypes confirm the predicted trend.[33,48–52] For the high doping levels often found in SiC the Schottky barrier height is usually lower than given by Eq. (1).[49]

The available data for the electron affinity are listed in Table I and show a similar scatter as the work function. None of these studies meets the current state of the art in surface preparation and characterization. However, the data for different polytypes show an increasing electron affinity with decreasing band gap, which gives within error limits a constant ionization energy of 6.35±0.25 eV.[37]

An alternative way to determine the ionization energy uses the work function and the energy of the VBM relative to the Fermi energy. The work functions obtained in this work for the $(\sqrt{3}\times\sqrt{3})R30°$ surfaces of 4H- and 6H-SiC are 4.74±0.06 eV and 4.89±0.05 eV, respectively. Table II gives an average value for the valence-band maximum 2.15

± 0.20 eV below the Fermi level independent of polytype and temperature, which yields an ionization energy of 6.9 ± 0.2 eV (7.0$\pm$0.2 eV). With the band gap of 3.26 eV (3.03 eV) we obtain an electron affinity of 3.6$\pm$0.2 eV for 4*H* (4.0$\pm$0.2 eV for 6*H*) within the range of the data of Table I. Our results show the right trend with band-gap energy and are compatible with a constant ionization energy around 7.0 eV. The smaller value of 6.35 eV found in the literature[37] could be attributed to a less-defined surface preparation, which generally leads to lower values for the work function and ionization energy. The value $\xi = 5.7$ eV reported in Ref. 36 for well-prepared 6*H*-SiC(0001) surfaces was obtained assuming that the occupied surface state is the valence-band maximum.[7] Using the data from Table II this energy has to be raised by $\sim$1.1 eV, which yields an ionization energy of 6.8 eV, comparable to our value. For the 4*H*-SiC(0001)(3×3) surface we obtain an ionization energy of 6.7$\pm$0.2 eV and an electron affinity of 3.4$\pm$0.2 eV using the work function from Table I and the energy of the VBM at $E_F - 2.0 \pm 0.2$ eV.[4,17,18]

B. Surface states

1. Occupied Mott-Hubbard state

On the $(\sqrt{3}\times\sqrt{3})R30°$ reconstructed surface the occupied Mott-Hubbard state is found in UPS as well as in 2PPE. The energy is 1.0 eV below the Fermi level in very good agreement with the previous reports listed in Table II. In 2PPE the excitation from the occupied Mott-Hubbard state takes place via direct absorption of two uv photons. Accordingly the intensity rises quadratically with the uv power. Upon variation of the photon energy by $3\Delta h\nu$ the kinetic energy of the electrons changes by the double amount $6\Delta h\nu$. The transition is observed only with *p*-polarized light, as expected for a totally symmetric state.[26] The dispersion away from $k_\parallel = 0$ is downward in agreement with UPS (Fig. 3).

With additional IR light the direct excitation of the occupied Mott-Hubbard state is possible by absorption of one uv and one ir photon. The peak observed around 1.0 eV kinetic energy would be a candidate for this transition. However, an exact analysis of the data reveals for the transition an energy $\sim$0.12 eV higher than expected. The variation of the kinetic energy is proportional to $(3.0\pm0.2)\Delta h\nu$ and significantly smaller than the expected $4\Delta h\nu$ for the occupied Mott-Hubbard state. The small energy differences are significant, since the appropriate transitions appear in the same spectrum (see Fig. 4). The unusual uv power dependence with an exponent of 1.7 also contradicts the assignment of this peak to the occupied Mott-Hubbard state excited simultaneously by one uv and one ir photon. We cannot exclude that this process contributes to the observed peak, but the major part must be of different origin.

2. Unoccupied Mott-Hubbard state

We assign the structure at $\sim$2 eV kinetic energy in the spectra of Fig. 5 to the unoccupied Mott-Hubbard state. According to the energetic position it is excited by two uv photons. This is supported also by the quadratic dependency of the count rate on the uv power. An excitation is not possible for purely *s*-polarized light. The dispersion is negative as observed for the other surface states. At emission angles of approximately 18° the structure becomes more intensive and a variation of the kinetic energy proportional to $\sim 3\Delta h\nu$ is observed as expected for an intermediate state. The intensity of the structure around 2 eV kinetic energy is similar to that of the occupied Mott-Hubbard state under comparable excitation with only uv light. The energy 1.45$\pm$0.1 eV above E_F is somewhat higher than the values in the range of 1.0$\pm$0.1 eV reported by other experimental studies (see Table II). However, the resulting Mott-Hubbard splitting of 2.4$\pm$0.1 eV is compatible with other reports, which usually combine results from two different experimental techniques. In 2PPE both peaks appear in the same spectrum though with rather small intensity.

There are two experimental findings that are at variance with the assignment of the peak around 2 eV kinetic energy to the unoccupied Mott-Hubbard state: (i) In experiments with time delay between two uv pulses no lifetime could be determined within the resolution of $\sim$100 fs. In comparison to Si(100) ($>$100 ps, Refs. 55 and 56) an even longer lifetime could be expected for the surface conduction band on SiC with small dispersion and consequently strong localization. The higher defect density on SiC can explain the short lifetime only unsatisfactorily, since the strong localization limits also the charge carrier diffusion to defect atoms. The degeneracy with conduction-band states (Fig. 1) might permit a fast decay of the unoccupied Mott-Hubbard band into bulk states. The excitonic state discussed in Sec. IV B 4 provides an additional decay channel. (ii) One would expect the intensity to decrease for off-normal emission with increasing component of the polarization vector normal to the surface in contrast to the observation. The occupied Mott-Hubbard state shows the behavior expected for a p_z-derived band and it should be identical for the unoccupied partner.

3. Occupied $3p_{x,y}$ surface state

Band-structure calculations[4,10,26,27] show an occupied surface-state band derived from $3p_x$ and $3p_y$ orbitals of the Si adatoms at an energy 0.5–1.0 eV below the valence-band maximum. This state has not been identified in photoemission experiments presumably due to the strong emission attributed to the valence bands in this energy range. With typical uv photon energies around 4.6 eV this state would be excited into an intermediate state around $E_F + 1.6$ eV. This energy is close to the peak assigned to the unoccupied Mott-Hubbard state in the preceding section. The $3p_{x,y}$ surface bands could therefore contribute to the broad peak seen around 2 eV kinetic energy and provide an explanation for the somewhat higher energy of the unoccupied Mott-Hubbard state found in our work compared to other studies. The so far unexplained intensity increase for off-normal emission is compatible with a $3p_{x,y}$ orbital character. In addition an enhancement by resonant transitions from the $3p_{x,y}$ bands into the unoccupied Mott-Hubbard band might be possible at certain angles.

4. Mott-Hubbard exciton

The feature not yet explained is the strong emission around 1 eV kinetic energy. The experimental findings indicate an unoccupied state at $E_F+0.75$ eV, which is totally symmetric with respect to the surface normal. This would be compatible with the unoccupied Mott-Hubbard state but the energy is significantly lower than the values in the range of 1.0 ± 0.1 eV reported by other experimental studies (see Table II). The occupied Mott-Hubbard state could serve as initial state, but it is about 0.12 eV lower in energy and it should dominate the 2PPE spectrum for off-resonant excitation.[57] Furthermore, it should be possible to excite the unoccupied Mott-Hubbard state without ir light by uv light only from the valence band. There is no indication for this peak in the experimental data for uv excitation only (see Figs. 5, 8, and 9).

The peak is observed with excitation by two uv photons and one ir photon and has strong intensity in the spectra. Three-photon photoemission processes are observed only in rare cases with rather low intensity.[58–60] An explanation of the observed behavior can only be the buildup of a large population in an intermediate state in combination with a long lifetime. Electrons in this state have an excitation energy considerably below the band gap. Relaxation is therefore only possible by recombination with holes, which explains the buildup of the population with a lifetime longer than the time between two laser pulses.

The energy of the state observed in two-photon photoemission is lower than any single-particle state found in band-structure calculations or inverse photoemission. An exciton is a common many-particle excitation found in semiconductors. In a simple picture with negligible hopping an electron is excited from one atom to a neighboring atom. This creates a doubly occupied site that expends the on-site Hubbard energy U. We can estimate the excitonic binding energy from the Coulomb attraction between the electron and the hole sitting at a distance of 5.32 Å between two neighboring Si adatoms in the $(\sqrt{3}\times\sqrt{3})R30°$ structure. Using an average dielectric constant at the surface between the bulk and vacuum values[61] of $(\varepsilon_\infty+1)/2$ we obtain an excitonic binding energy of 0.72 eV in good agreement with the experimental energy lowering of 0.7 ± 0.2 eV with respect to the unoccupied Mott-Hubbard state.

The exciton formation requires the creation of an electron and a hole, which is the first step in the 2PPE process. It cannot be formed by direct optical excitation, because the wave functions of the occupied and unoccupied Mott-Hubbard bands are identical, leading to a vanishing dipole matrix element. The difference is in the spin configuration, which cannot be altered by optical excitation. In any case the energy lowering would not be observable in a simple 2PPE experiment, because the final state is a one-hole state. The energy gained by the formation of the exciton in the first step is lost by the breakup in the second step.

The electron and hole created after the initial photon absorption have to scatter and loose energy before the exciton formation. Because the exciton is the quasiparticle excitation with the lowest energy at the SiC(0001)$(\sqrt{3}\times\sqrt{3})R30°$ surface it is very likely that electrons and holes end up in an excitonic bound state before they recombine. One possible process involving mainly surface states is sketched in Fig. 10.

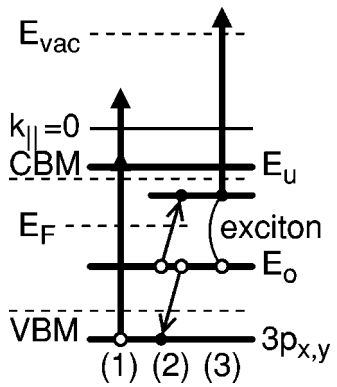

FIG. 10. Energy diagram illustrating the formation of an exciton on the SiC(0001)$(\sqrt{3}\times\sqrt{3})R30°$ surface. (1) The hole in the $3p_{x,y}$ band is created after absorption of an uv plus an ir photon. (2) The recombination in an Auger-like process leads to the formation of the exciton. (3) A second uv photon is used to detect the exciton.

(1) An electron from the occupied $3p_{x,y}$ surface state is excited into the conduction band. For the SiC(0001)$(\sqrt{3}\times\sqrt{3})R30°$ surface the conduction-band minimum at $k_\parallel=0$ is $\sim$4.5 eV above the valence-band maximum.[6,62,63] The $3p_{x,y}$ band is $\sim$0.7 eV below the valence-band maximum.[4,10,26,27] The excitation energy of >5.2 eV cannot be provided by a uv photon ($3h\nu<4.9$ eV in this work) only and requires at least one uv plus one ir photon. This two-photon absorption process might be enhanced by transitions into surface bands near the conduction-band minimum at $k_\parallel=0$.[64]

(2) The hole in the $3p_{x,y}$ surface state is filled by an electron from the occupied Mott-Hubbard band. The available energy of $\sim$1.7 eV is used to excite a second electron from the occupied Mott-Hubbard band into the unoccupied Mott-Hubbard band in an Auger-like process. The probability for this process is enhanced if the excitation involves neighboring sites favoring the formation of the exciton. The extra hole in the Mott-Hubbard bands does not have to be bound to the exciton.[65] The process is not specific to the $3p_{x,y}$ surface states as initial states. However, the localization of these states on the adatoms ensures a high overlap with the $3p_z$ states forming the Mott-Hubbard bands. The $3p_{x,y}$ surface states happen to be just at the right energy for the Auger-like recombination process. It should be mentioned that the spins of the $3p_{x,y}$ surface and $3p_z$ Mott-Hubbard states are correlated,[10] which might favor the spin configuration of the exciton.

(3) The second uv photon breaks up the exciton and lifts the electron above the vacuum energy. The final state leaves the surface with a hole in the occupied Mott-Hubbard band. The energy of the exciton corresponds to the difference between the two Mott-Hubbard bands reduced by the excitonic binding energy. The kinetic energy of the emitted electron is therefore lowered by the excitonic binding energy compared to direct ionization of the unoccupied Mott-Hubbard band.

The energy plotted in Fig. 10 is the final state energy observed in the experimental spectrum minus the uv photon energy used for ionization and should not be confused with the energy of the excitonic two-particle excitation.

The high intensity of the observed peak could be attributed to a long lifetime of the exciton. Radiative decay is forbidden, because it would require a spin flip. In the absence of electronic excitations at the SiC(0001)$(\sqrt{3}\times\sqrt{3})R30°$ surface with energies below the exciton energy of 1.75 eV, the recombination has to involve defects. It is therefore conceivable, that the lifetime could be longer than the separation of 12 ns between two laser pulses. This would prohibit the measurement of the lifetime with our setup. On the other hand such a long lifetime would lead to an extremely narrow linewidth in contrast to the observation of a peak width of 0.4 eV. Possible explanations could be contributions of different excitonic states[66] or surface inhomogeneities.

An additional factor contributing to the high intensity observed is the localized nature of the exciton. The process sketched in Fig. 10 is not limited to $k_{\parallel}=0$. According to the small dispersion of the $3p_{x,y}$ band, holes throughout the surface Brillouin zone may contribute to the exciton formation. Due to the small kinetic energies and good angular resolution only $\sim 1/1000$ of the surface Brillouin zone is sampled in the 2PPE spectra. This could enhance the intensity of the exciton peak relative to other peaks by up to three orders of magnitude and would also provide an explanation of the high intensity. As sketched in the energy diagram of Fig. 10 the uv photon energy would be large enough to excite from the $3p_{x,y}$ into the conduction-band minimum. However, uncertainties in the dispersion and energies of the $3p_{x,y}$ band and matrix-element effects might render this absorption improbable. Experiments with higher photon energies would be desirable to enhance the excitation of the $3p_{x,y}$ states. However, increased direct one-photon photoemission will hamper such measurements.

A unique characteristic of the Auger-like process is the absence of a primary excitation in the Mott-Hubbard bands. Adding or subtracting an electron directly to or from these bands should always be possible with uv light only and does not require the additional ir photon needed in the experimental circumstances. In direct excitation of the Mott-Hubbard bands the complementary quasiparticle would be in bulk bands and would require several scattering processes for the charges to rejoin at the surface to form the exciton (see Fig. 10). The Auger-like process requires only the creation of a hole in the $3p_{x,y}$ band to form the exciton in one step. Other mechanisms of exciton formation such as trapping of electrons from the conduction-band minimum by holes in the lower Mott-Hubbard band cannot be excluded. On the SiC(0001)$(\sqrt{3}\times\sqrt{3})R30°$ surface the time scale and energetics of formation and decay could not be resolved for SiC in contrast to Si(100).[55,56]

V. SUMMARY AND OUTLOOK

We have identified an excitonic excitation between the Mott-Hubbard states in two-photon photoemission experiments. It is formed in an Auger-like process involving $3p_{x,y}$ holes and the $3p_z$ states on the Si adatoms of the SiC(0001) $(\sqrt{3}\times\sqrt{3})R30°$ surface. It would be interesting to extend the studies to higher photon energies, which would allow a direct excitation from the $3p_{x,y}$ bands into the conduction band with uv light alone, eliminating the two-photon absorption process. This should enhance the signal from the exciton drastically and new effects could appear in the Mott-Hubbard bands at high excitation densities. A prerequisite would be a long lifetime in the Mott-Hubbard bands, which should be confirmed by time-resolved measurements involving a delay between the two uv photons with simultaneous ir illumination.

ACKNOWLEDGMENTS

We are indebted to Igor L. Shumay and Wang Jinxiong for their expert help with the laser system. We thank Michael Rohlfing for stimulating and helpful discussions on Mott-Hubbard bands. This work was supported by the Deutsche Forschungsgemeinschaft through SFB 292.

*Electronic address: fauster@physik.uni-erlangen.de

[1] G. Pensl and R. Helbig, in *Festkörperprobleme/Advances in Solid State Physics*, edited by U. Rössler (Vieweg, Braunschweig, 1990), Vol. 30, p. 133.
[2] U. Starke, Phys. Status Solidi B **202**, 475 (1997).
[3] J.-M. Themlin, I. Forbeaux, V. Langlais, H. Belkhir, and J.-M. Debever, Europhys. Lett. **39**, 61 (1997).
[4] J. Furthmüller, F. Bechstedt, H. Hüsken, B. Schröter, and W. Richter, Phys. Rev. B **58**, 13712 (1998).
[5] J. E. Northrup and J. Neugebauer, Phys. Rev. B **57**, R4230 (1998).
[6] M. Rohlfing and J. Pollmann, Phys. Rev. Lett. **84**, 135 (2000).
[7] L. I. Johansson, F. Owman, and P. Mårtensson, Surf. Sci. **360**, L478 (1996).
[8] V. Ramachandran and R. M. Feenstra, Phys. Rev. Lett. **82**, 1000 (1999).
[9] J. R. Ahn, S. S. Lee, N. D. Kim, C. G. Hwang, J. H. Min, and J. W. Chung, Surf. Sci. **516**, L529 (2002).
[10] V. I. Anisimov, A. E. Bedin, M. A. Korotin, G. Santoro, S. Scandolo, and E. Tosatti, Phys. Rev. B **61**, 1752 (2000).
[11] Th. Fauster, in *Solid-State Photoemission and Related Methods*, edited by W. Schattke and M. Van Hove (Wiley-VCH, Weinheim, 2003).
[12] M. Weinelt, J. Phys.: Condens. Matter **14**, R1099 (2002).
[13] M. J. Bozack, Phys. Status Solidi B **202**, 549 (1997).
[14] A. Schäfer, I. L. Shumay, M. Wiets, M. Weinelt, Th. Fauster, E. V. Chulkov, V. M. Silkin, and P. M. Echenique, Phys. Rev. B **61**, 13159 (2000).
[15] T. Hertel, E. Knoesel, A. Hotzel, M. Wolf, and G. Ertl, J. Vac. Sci. Technol. A **15**, 1503 (1997).
[16] L. I. Johansson, F. Owman, P. Mårtensson, C. Persson, and U. Lindefelt, Phys. Rev. B **53**, 13803 (1996).
[17] H. Hüsken, B. Schröter, and W. Richter, Surf. Sci. **407**, L676 (1998).

[18] L. S. O. Johansson, L. Duda, M. Laurenzis, M. Krieftewirth, and B. Reihl, Surf. Sci. **445**, 109 (2000).
[19] P.-A. Glans and L. I. Johansson, Surf. Sci. **465**, L759 (2000).
[20] The spectra are normalized by the square of the uv power for better comparison of the two-photon photoemission features.
[21] Th. Fauster and W. Steinmann, in *Photonic Probes of Surfaces*, edited by P. Halevi (North-Holland, Amsterdam, 1995), Vol. 2 of *Electromagnetic Waves: Recent Developments in Research*, p. 347.
[22] P. Mårtensson, F. Owman, and L. I. Johansson, Phys. Status Solidi B **202**, 501 (1997).
[23] C. Cobet, K. Wilmers, T. Wethkamp, N. V. Edwards, N. Esser, and W. Richter, Thin Solid Films **364**, 111 (2000).
[24] The data can be fitted by a linear combination of first- and second-order processes as well: $I=aP+bP^2$. The exponent of the power law fit $I\propto P^{\mu}$ is in good approximation given by $\mu=1+1/(1+0.2\ \mathrm{mW}^{-1}\ a/b)$.
[25] We did not check the dependence on ir power. Therefore, the absorption of several ir photons cannot be excluded, but a process of even higher order seems unlikely.
[26] J. E. Northrup and J. Neugebauer, Phys. Rev. B **52**, R17001 (1995).
[27] M. Sabisch, P. Krüger, and J. Pollmann, Phys. Rev. B **55**, 10561 (1997).
[28] J. A. Dillon Jr., R. E. Schlier, and H. E. Farnsworth, J. Appl. Phys. **30**, 675 (1959).
[29] L.I. Kaisheva, Fiz. Tver. Tela **14**, 2438, (1972) [Sov. Phys. Solid State **14**, 2108 (1973)].
[30] K. W. Frese Jr., J. Vac. Sci. Technol. **16**, 1042 (1979).
[31] J. Pelletier, D. Gervais, and C. Pomot, J. Appl. Phys. **55**, 994 (1984).
[32] D. Alok, P. K. McLarty, and B. J. Baliga, Appl. Phys. Lett. **64**, 2845 (1994).
[33] L. M. Porter and R. F. Davis, Mater. Sci. Eng., B **34**, 83 (1995).
[34] A. L. Syrkin, A. N. Andreev, A. A. Lebedev, M. G. Rastegaeva, and V. E. Chelnokov, J. Appl. Phys. **78**, 5511 (1995).
[35] A. L. Syrkin, A. N. Andreev, A. A. Lebedev, M. G. Rastegaeva, and V. E. Chelnokov, Mater. Sci. Eng., B **29**, 198 (1995).
[36] V. van Elsbergen, T. U. Kampen, and W. Mönch, J. Appl. Phys. **79**, 316 (1996).
[37] J. Kuriplach, M. Šob, G. Brauer, W. Anwand, E.-M. Nicht, P. G. Coleman, and N. Wagner, Phys. Rev. B **59**, 1948 (1999); the ionization energy is called work function in this work.
[38] S. Kennou, J. Appl. Phys. **78**, 587 (1995).
[39] S. Kennou, A. Siokou, I. Dontas, and S. Ladas, Diamond Relat. Mater. **6**, 1424 (1997).
[40] T. Jikimoto, J. L. Wang, T. Saito, M. Hirai, M. Kusaka, M. Iwami, and T. Nakata, Appl. Surf. Sci. **130-132**, 593 (1998).
[41] C. Benesch, M. Fartmann, and H. Merz, Phys. Rev. B **64**, 205314 (2001).
[42] L. I. Johansson, F. Owman, and P. Mårtensson, Phys. Rev. B **53**, 13793 (1996).
[43] P.-A. Glans, T. Balasubramanian, M. Syväjärvi, R. Yakimova, and L. I. Johansson, Surf. Sci. **470**, 284 (2001).
[44] L. I. Johansson, F. Owman, and P. Mårtensson, Surf. Sci. **360**, L483 (1996).
[45] F. S. Tautz, S. Sloboshanin, U. Starke, and J. A. Schaefer, Surf. Sci. **470**, L25 (2000).
[46] C. Virojanadara and L. I. Johansson, Surf. Sci. **505**, 358 (2002).
[47] J. Schardt, J. Bernhardt, U. Starke, and K. Heinz, Phys. Rev. B **62**, 10335 (2000).
[48] W. Mönch, in *Control of Semiconductor Interfaces*, edited by I. Ohdomari, M. Oshima, and A. Hiraki (Elsevier, Amsterdam, 1994), p. 169.
[49] A. L. Syrkin, J. M. Bluet, G. Bastide, T. Bretagnon, A. A. Lebedev, M. G. Rastegaeva, N. S. Savkina, and V. E. Chelnokov, Mater. Sci. Eng., B **B46**, 236 (1997).
[50] A. Itoh and H. Matsunami, Phys. Status Solidi A **162**, 389 (1997).
[51] W. J. Lu, D. T. Shi, A. Burger, and W. E. Collins, J. Vac. Sci. Technol. A **17**, 1182 (1999).
[52] S. Y. Davydov, A. A. Lebedev, O. V. Posrednik, and Y. M. Tairov, Fiz. Tekh. Poluprovdn. **35**, 1437 (2001) [Semiconductors **35**, 1375 (2001)],
[53] I. Forbeaux, J.-M. Themlin, V. Langlais, L. M. Yu, H. Belkhir, and J.-M. Debever, Surf. Rev. Lett. **5**, 193 (1998).
[54] L. Duda, Ph.D. thesis, Universität Dortmund (2000), URL: http://eldorado.uni-dortmund.de/FB2/ls1/forschung/2000/Duda.
[55] M. Kutschera, Ph.D. thesis, Universität Erlangen-Nürnberg (2001).
[56] M. Weinelt, M. Kutschera, Th. Fauster, and M. Rohlfing (unpublished).
[57] K. Boger, M. Roth, M. Weinelt, Th. Fauster, and P.-G. Reinhard, Phys. Rev. B **65**, 075104 (2002).
[58] P. G. Strupp, P. C. Stair, and E. Weitz, Surf. Sci. **290**, L699 (1993).
[59] I. Kinoshita, T. Anazawa, and Y. Matsumoto, Chem. Phys. Lett. **259**, 445 (1996).
[60] S. Ogawa and H. Petek, Surf. Sci. **363**, 313 (1996).
[61] M. Rohlfing and J. Pollmann, Phys. Rev. B **63**, 125201 (2001), and private communication.
[62] B. Wenzien, P. Käckell, F. Bechstedt, and G. Cappellini, Phys. Rev. B **52**, 10897 (1995).
[63] I. S. Gorban' and A. P. Krokhmal', Fiz. Tekh. Poluprovdn. **35**, 1299 (2001) [Semiconductors **35**, 1242 (2001)].
[64] M. Sabisch, P. Krüger, A. Mazur, and J. Pollmann, Surf. Rev. Lett. **5**, 199 (1998).
[65] The Coulomb attraction and repulsion of the extra hole by the electron and hole of the exciton cancel depending on the local configuration.
[66] M. E. Simón, A. A. Aligia, C. D. Batista, E. R. Gagliano, and F. Lema, Phys. Rev. B **54**, R3780 (1996).